Clays and Clay Minerals, Vol. 60, No. 5, 535–552, 2012.

RIETVELD REFINEMENT OF DISORDERED ILLITE-SMECTITE MIXED-LAYER STRUCTURES BY A RECURSIVE ALGORITHM. II: POWDER-PATTERN REFINEMENT AND QUANTITATIVE PHASE ANALYSIS

KRISTIAN UFER[1,3,*], REINHARD KLEEBERG[1], JÖRG BERGMANN[2,†] AND REINER DOHRMANN[3]

[1] Institute of Mineralogy, TU Bergakademie Freiberg, Brennhausgasse 14, 09596 Freiberg, Germany
[2] Ludwig-Renn-Allee 14, 01217 Dresden, Germany
[3] BGR/LBEG, Stilleweg 2, 30655 Hannover, Germany

Abstract—X-ray diffraction (XRD) of powdered materials is one of the most common methods used for structural characterization as well as for the quantification of mineral contents in mixtures. The application of the Rietveld method for that purpose requires structure models for each phase. The recursive calculation of structure factors was applied here to the Rietveld refinement of XRD powder patterns of illite-smectite (I-S) minerals. This approach allowed implementation of stacking disorder in structural models. Models for disordered stacking of *cis*-vacant and *trans*-vacant dioctahedral 2:1 layers as well as rotational disorder were combined with models for mixed layering of illitic and smectitic layers.

The *DIFFaX* code was used to simulate non-basal (*hk*) reflections of illites with different degrees of disorder. Rietveld refinements of these simulated patterns were used to evaluate the application of this new approach. A model describing rotational disorder ($n\cdot120^{o}$ and $n\cdot60^{o}$ rotations) and mixed layering of *cis*-vacant and *trans*-vacant dioctahedral layers was tested. Different starting parameters led to identical results within the ranges of standard deviations and confirmed the stability of the automatic refinement procedure. The influence on the refinement result of an incorrect choice of fixed parameters was demonstrated.

The *hk* model was combined with models describing the basal reflections of disordered I-S and tested on measured data. A glauconitic mineral (Urkut, Hungary), an ordered I-S (ISCz-1, a special clay in the Source Clays Repository of The Clay Minerals Society), and a dioctahedral I-S (F4, Füzérradvány, Hungary) were used as test substances. Parameters describing the mixed layering of illitic and smectitic layers were compared with the results from refinements of oriented mounts and showed good agreement. A pattern of a physical mixture of an I-S mineral and a turbostratically disordered smectite was analyzed in order to test the new approach for application in quantitative phase analysis. The quantitative Rietveld phase analysis results were found to be satisfactory.

Key Words—*BGMN*, *DIFFaX*, Illite-smectite, Quantitative Phase Analysis, Rietveld Refinement, Stacking Faults.

INTRODUCTION

Mixed-layered minerals are extremely common in nature, and a large majority of these include expandable layers which cause problems in the refinement of structure parameters because they correspond to random rotations and translations of the layers relative to each other. The sequence of expandable and non-expandable layers may also be irregular.

A second difficulty is related to the frequent occurrence of well defined stacking faults in the structure fragments separated by these expandable layers. Both random and well defined stacking defects modify the intensity distribution and the usual Rietveld codes are rendered useless for structure refinement. The aim of the present study was to demonstrate that the Rietveld method in combination with a recursive calculation of structure factors (Treacy *et al.*, 1991) can be used for the determination of structural parameters as well as for quantitative phase analysis (QPA) of mixtures containing disordered mixed layers. Up to now, the use of three-dimensional patterns for structure modeling and QPA of mixtures containing disordered mixed layers such as clay minerals was restricted to specialized software codes such as *Sybilla 3D* (Chevron ETC propriety software, based on Drits and Sakharov (1976) and Drits and Tchoubar (1990)) with a limited number of structure models or to Rietveld codes which can handle lists of structure factors instead of structural models (Taylor and Matulis, 1994; Scarlett and Madsen, 2006). The latter approach requires pure standard materials for calibration and suffers from the lack of correction tools to eliminate the inevitable effects of preferred orientation. These limitations cause inflexibility. The present work combines a structure-based modeling of mixed layers with the advantages and tools of a Rietveld refinement.

Hydrous phyllosilicate minerals can form sequences of different kinds of layers, such as illite-smectite (I-S) or glauconite-smectite (G-S). These stackings can be described using the concept of "fundamental particles"

* E-mail address of corresponding author:
kristian.ufer@gmx.de
† Deceased
DOI: 10.1346/CCMN.2012.0600508

(Nadeau *et al.*, 1984) or so-called "MacEwan crystallites" (MacEwan, 1956). Fundamental particles are stacks of two or more 2:1 layers with non-hydrated interlayer cations (mostly K^+) in well defined positions and hydrated cations on their outer interfaces. The layers are rotated or translated parallel to each other by well defined angles or translation vectors. Two kinds of rotational arrangements are described, the first contains rotations of $n{\cdot}120^o$ only (n = 0, 1, or 2) and the second shows $n{\cdot}60^o$ rotations also (n = 1, 3, or 5). The center of rotation is the interlayer cation, which is located above the ditrigonal cavity of the tetrahedral sheet. The $n{\cdot}120^o$ rotations lead to an octahedral coordination of the interlayer cation, while $n{\cdot}60^o$ rotations produce a prismatic arrangement. The two tetrahedral sheets of a 2:1 layer are translated parallel to the layer by $\sim -1/3{\cdot}a$. The stacking of illite layers is, for that reason, always related to a translation, the direction of which depends on the rotation of the layers relative to each other. Such stacking can be described as ordered polytypes if these rotations and translations occur regularly, *e.g.* 1*M* or $2M_1$ illites. In other cases these displacements occur disordered and the stacking can only be described statistically by probabilities. Additional disorder may arise from the coexistence of *cis*-vacant and *trans*-vacant 2:1 layers (Tsipursky and Drits, 1984). Translations and/or rotations of the layers parallel to each other or different octahedral vacancies do not change the z coordinate of the atomic positions. These disorder effects in the fundamental particles consequently have no influence on the basal reflections. The kind of disorder can only be identified by diagnostic peak broadenings or shiftings of the non-basal reflections. The highest degree of disorder is reached when all rotations are equiprobable.

Turbostratic disorder occurs in I-S in addition to the rotations or translations by well defined angles or translation vectors. This kind of disorder was first described by Warren (1941) as random rotations and translations of the layers relative to each other, thus preventing coherent scattering of the units which are separated by that. Basal reflections are again unaffected by this kind of stacking. Structural units which are oriented turbostratically relative to each other produce non-basal reflections which are identical to those produced by separate crystallites. Reynolds (1992) suggests that turbostratic disorder occurs only at the smectitic junctions between fundamental particles and is restricted to that. Accordingly, the coherent scattering units producing the non-basal reflections are the illite fundamental particles. The non-basal reflections of an I-S can be described by models concerning only *cv* and *tv* illitic layers with $n{\cdot}60^o$ or $n{\cdot}120^o$ rotations. This description is still valid even if the fundamental particles show internal turbostratic defects, because Reynolds (1992) established that the non-basal reflections are not affected by the nature of the outer surface of the coherent scattering units. Internal turbostratic disorder may only subdivide the fundamental particles into smaller coherent diffracting units. Accordingly, the three-dimensional structure of the smectitic interlayer is not detectable by powder diffraction. Only the z coordinate is accessible by the examination of the basal reflections.

The concept of regarding an I-S stack as a MacEwan crystallite can be used to describe the stacking of illitic and smectitic layers and to model the diffraction of the basal reflections. MacEwan crystallites are sequences of sub-units, consisting of one-half each of two superimposed 2:1 layers with either an illitic or a smectitic interlayer (Altaner and Ylagan, 1997). The order of the stacking of layers with different spacings influences the positions and broadenings of intensity maxima of the basal reflections. The peaks show a rational series if all sub-units have the same thickness or if the stack consists of a regular interstratification of layers of different thickness forming a perfect supercell. In the case of a disordered stacking of illitic and smectitic interlayers (in different hydration states), the series of peaks is non-rational and individual peaks show different broadenings (Méring, 1949). Models to describe the basal diffraction of I-S or G-S were presented in the first part of this study (Ufer *et al.*, 2012). These models are combined here with a model for the non-basal reflections to describe the whole powder pattern. The approach of using two different models is justified by the concept of considering I-S on the one hand as MacEwan crystallites which influence the basal reflections and on the other hand as fundamental particles which scatter coherently but independently from each other like random oriented units according to the non-basal reflections.

MATERIALS AND METHODS

The capabilities and limitations of the recursive approach were first demonstrated by the Rietveld refinement of simulated data. The software code *DIFFaX* (Treacy *et al.*, 1991) was used for these simulations. The results of *DIFFaX* simulations and Rietveld refinements using the *BGMN* software (Bergmann *et al.*, 1998) with the same structural parameters naturally give almost identical results (Ufer *et al.*, 2008a; 2012), because both programs use the same mathematical description of diffraction. The simulated data contained two different series, each varying one of the statistical parameters to describe the stacking disorder. Rietveld refinement tests were carried out on these simulated data with different starting parameters and with incorrect fixed parameters, used in order to highlight the relevance of the structure model. Basal reflections were not considered in this first step.

The same disorder model was applied in refinements on measured data in the next step, using the testing materials which were introduced by Ufer *et al.* (2012).

https://doi.org/10.1346/CCMN.2012.0600508 Published online by Cambridge University Press

Suitable structure models to describe the basal reflections were chosen according to the results of Ufer *et al.* (2012). These models were refined with the same starting values and limits as in the refinements using the measured data of the oriented mounts.

Simulation by DIFFaX

The simulation software *DIFFaX* requires the input of structural data for the generation of powder patterns. The atomic positions for the illitic 2:1 layer were taken from Drits *et al.* (2006). The original coordinates were recalculated for an orthogonal unit cell with the K atom at the origin (Table 1a). The *cis*-vacant (*cv*) 2:1 layer structures were calculated from the *trans*-vacant (*tv*) layer structures according to Tsipursky and Drits (1984). Typical values were chosen for the occupancies of the positions and the Debye-Waller factor of all atoms was set to zero. The lattice constants were set to a = 5.193 Å and b = 8.995 Å.

DIFFaX does not allow the definition of rotations between given layer structures, only translations. Each orientation of each layer type (*cv* and *tv*) was consequently defined as an additional layer type to overcome this limitation. The choice of the a and b lattice constants allows definition of $n\cdot60^\circ$ rotations within the same unit cell without distortions, because the ratio $b/a = \sqrt{3}$ results from the pseudo-hexagonal symmetry of the tetrahedral and octahedral sheets. Altogether, 12 layer structures were defined to account for all $n\cdot60^\circ$ rotations of both *cv* and *tv* layers. The layers are shifted parallel to each other in the a direction by $t_x \cdot a = -0.2999 \cdot a$ (*cv*) or $t_x \cdot a = -0.4008 \cdot a$ (*tv*) to fit the K^+ ion in the ditrigonal cavity of the sandwiching layers. These translation vectors also had to be rotated for all layer rotations.

The following disorder phenomena for the simulation of the non-basal reflections were considered: interstratification of *cis*-vacant and *trans*-vacant layer types, $n\cdot120^\circ$ rotational disorder, and the additional occurrence of $n\cdot60^\circ$ rotations (n: odd number). The statistical parameter, *pcv*, describes the probability of a layer being a *cis*-vacant structure. As a consequence, the probability that a layer has *trans*-vacant structure is $ptv = 1 - pcv$. Rotational disorder is described by the two parameters $p0$ and $p60120$. Parameter $p0$ is the probability that the following layer is rotated by 0º. The case $p0 = 1$ describes perfect 1*M* stacking. The parameter $p60120$ controls whether a non-0º rotation is a 120º/240º rotation or a 60º/180º/300º rotation. The value of $p60120$ is equal to zero if all non-0º rotations are 120º/240º rotations. These two rotations are regarded as equiprobable and the probabilities are $p120 = p240 = (1 - p60120)\cdot(1 - p0)/2$. The probability for 60º, 180º, and 300º rotations are $p60 = p180 = p300 = p60120\cdot(1 - p0)/3$.

Two different series of patterns were calculated, varying $p0$ and *pcv*. All simulation parameters are listed together with the refinement results (Table 2, 3). Only non-basal reflections were examined in these simulations. Using *DIFFaX*, calculation of a powder pattern without basal reflections is impossible, but calculation of the basal reflections separately with the same structural data and subtraction of the intensity from the powder pattern are possible. The *DIFFaX* calculations were performed for a monochromatic wavelength of 1.789007 Å ($CoK\alpha_1$) and a Lorentzian-shaped instrumental broadening with a constant full-width at half maximum of 0.6º. The resulting intensities were converted from a fixed divergence slit measurement (I_{fix}) to a measurement with variable divergence slit and constant irradiated sample length (I_{var}) by the relation $I_{var} = I_{fix}\cdot\sin\theta$. The simulated pattern covered a range from 5 to 80º2θ.

Background intensities and instrumental noise were added to the simulated intensities. These two contributions were extracted from data obtained on a well crystallized material (quartz) measured in a conventional experimental setting.

Rietveld refinements of simulated data

The *BGMN* software (Bergmann *et al.*, 1998) was used for recursive calculations in a Rietveld refinement. The *BGMN* code contains an interpreter language which allows the definition of additional functions and parameters. The manipulation of the complex structure factors of multiple-layer structures within one unit cell, the so-called sub-phases, is also possible. The use of an interpreter language permits a very flexible and transparent formulation without the need for hard coding. The recursive calculation of structure factors was described by Ufer *et al.* (2012). This description is universally valid although in the Ufer *et al.* (2012) study, only basal reflections of oriented mounts were calculated.

The refinement process is controlled *via* input text files. Once *BGMN* is started, a control file is read in calling the data file containing the observed data (simulated data in this case) and structure data files for each phase. The control file also defines the name and paths of three different output files. These files contain the diffraction patterns, a peak list and a list of the numerical results. The control file also includes structure-independent global parameters of the refinement. These parameters are correction parameters for sample displacement or zero point error, wavelength, refinement range, and the degree of a Lagrange polynomial to describe the background run.

The supercell which was used for the formulation of the disorder model was enlarged 100 times in the c direction and filled with only one layer per sub-phase. This procedure allows the calculation of the structure factors of the sub-phases periodically in the a and b directions and aperiodically in the c direction (Ufer *et al.*, 2008a). The use of an elongated and less than half filled unit cell for structure-factor calculation approximates the Fourier transformation of an aperiodic object.

https://doi.org/10.1346/CCMN.2012.0600508 Published online by Cambridge University Press

This is the mathematical interpretation of the diffraction process on a single layer. Periodicity in the *c* direction was reintroduced by the recursive calculations. Altogether twelve sub-phases had to be defined. The complex structure factor of each sub-phase is accessible as a modifiable parameter, which permits the mathematical description of the recursive structure-factor calculation of the disordered stack, as described by Treacy *et al.* (1991). The same disorder parameters as used for the simulations could so be introduced and refined.

Some extra functions were introduced in addition to this structure-factor calculation. The recursive treatment regards a stack as infinite and in the case of ordered stacking, a reflection becomes infinitely sharp though still having a finite area. This effect is problematic for a correct numerical integration even if the stacking is only slightly disordered. For this reason, an additional function was added to ensure a minimal peak-profile width of all reflections. A function for the calculation of correct densities from the partly filled unit cell and for a constant Lorentzian-shaped peak broadening was also introduced.

Each simulation was refined with a disorder model containing $n{\cdot}120^{\circ}$ and $n{\cdot}60^{\circ}$ rotations of *cv* and *tv* layers. The refineable parameters and the starting values for all refinements of the two series were mostly identical. Some parameters were varied or fixed incorrectly in further steps.

The probability of 0º rotations ($p0$) was initially set to 0.7 and refined between the limits 0.333 and 1. The probabilities *pcv* and $p60120$ were refined between 0 and 1 with 0.5 as starting values. The lattice constant *a* was also refined to the statistical parameters with the starting value 5.193 Å and the limits 5.1 Å and 5.3 Å. *b* is connected to *a via* the relationship $(b/a)^2 = 3$. The relative magnitude of the translation vector $-t_x$ was refined with the starting value 0.2999 for *cv* layers and 0.4008 for *tv* layers. The refinement ranges were 0.26−0.32 (*cv*) and 0.38−0.44 (*tv*).

No attempt was made to refine the atomic positions. Only the occupancies of Fe and K were refined with the starting values $p(\mathrm{Fe}) = 0.1$ and $p(\mathrm{K}) = 0.8$ in the ranges 0−0.7 (Fe) and 0.6−1 (K). A scaling factor and a constant peak-broadening factor were refined. The background was described by a 6th degree Lagrange polynomial.

Rietveld refinements of observed data

Three mixed layers with different degrees of long-range ordering (Reichweite R) were used in this work to test the three-dimensional Rietveld refinement: (1) randomly interstratified (R0) glauconite-smectite (G-S) from a Hungarian deposit referred to as 'Urkut'; (2) R1 ordered I-S from Slovakia referred to as 'ISCz-1' (a special clay mineral from the Source Clays Repository of The Clay Minerals Society); and (3) R3 ordered I-S from the Füzérradvány deposit, Hungary, referred to as 'F4.'

The structure model which was used to fit the non-basal reflections of the mixed layers was identical to that used above for simulated data. The atomic positions of the structural model for glauconite were derived from Sakharov *et al.* (1990) (Table 1b). The observed data also contained basal reflections of course. The disorder models used for the description of the basal reflections were given by Ufer *et al.* (2012). The main difference in the present study is that the scaling factor, the parameter for the correction of preferred orientation, and the occupation of K and Fe were defined as global parameters, *i.e.* identical and valid in both structure models for *hk* and 00l peaks. They were declared in the control file and passed to the structure models. These parameters were refined. The following parameters were refined individually for the one-dimensional I-S model: the thicknesses t_s of the smectitic layers in mono(1w)- and bi(2w)-hydrated states, the occupancies of the interlayer calcium cation $p(\mathrm{Ca})$ and the interlayer water molecules $p(\mathrm{H_2O})$, the distance of the water molecule to the midplane $d(\mathrm{H_2O})$ of the 2w state, the proportion of illitic layers *w*I, the probability $p1\mathrm{w}$ that a smectitic layer is in the monohydrated state, and the stacking probabilities *p*II, *p*III, and *p*IIII of the corresponding degree of Reichweite. *p*II is the probability that an I layer follows another I layer, *p*III is the probability that I follows a II pair, and *p*IIII is the probability that I follows a III triple stack. The maximum possible degree of ordering (mpdo) was assumed for the R3 model. A detailed description of all statistical parameters was given by Ufer *e al.* (2012).

The following chemical formulae of the testing materials were determined by Ufer *et al.* (2012):

Urkut: $Ca_{0.04}K_{0.71}Si_{3.91}Al_{0.09}(Al_{0.50}Fe_{0.83}Mg_{0.65})O_{10}(OH)_2$.

ISCz-1: $Ca_{0.09}K_{0.48}Si_{3.52}Al_{0.48}(Al_{1.70}Fe_{0.08}Mg_{0.24})O_{10}(OH)_2$.

F4: $Ca_{0.06}K_{0.67}Si_{3.41}Al_{0.59}(Al_{1.73}Fe_{0.03}Mg_{0.26})O_{10}(OH)_2$.

A mixture of the I-S sample F4 and a very smectite-rich bentonite was also prepared to evaluate the applicability of the models for quantitative phase analysis. The structural model for the description of the turbostratically disordered smectite used in this test mixture was described by Ufer *et al.* (2008b). A standard structural model was applied to the quartz impurities of all three samples. The ISCz-1 sample also contained traces of kaolinite which were ignored.

The *BGMN* software includes a fundamental-parameter approach for the modeling of the instrumental part of the peak profile (Cheary and Coelho, 1992). The instrument-dependent part of the diffraction profile is determined by a ray-tracing procedure prior to the refinement (Bergmann *et al.*, 1998). This profile information is stored in an additional file and called by the control file to be convoluted with the structure-dependent peak broadening. The zero point, the sample

https://doi.org/10.1346/CCMN.2012.0600508 Published online by Cambridge University Press

displacement error, and a 6th degree Lagrange polynomial for the description of the background run were refined as non-structural parameters.

Material pretreatment and XRPD analysis

Clay samples were disaggregated gently using deionized water and dispersed in an end-over-end shaker (24 h). Representative amounts of <2 μm fractions were collected and dried as described by Ufer *et al.* (2012). Different independent separation processes were performed for sample F4, due to its small clay content in the raw material.

A bentonite from Peru, S112, was also used to prepare a test mixture for a quantitative phase analysis. This bentonite is an almost pure smectite and only a small quartz impurity was detected. This impurity was quantified according to Ufer *et al.* (2008b) as <1 wt.%. Quantities, 1.000 g of F4 and 0.500 g of Ca-saturated S112, were mixed and homogenized by wet grinding with ethanol for 2 min in a McCrone mill. The resulting mixture contained 64 wt.% I-S, 33 wt.% smectite, and 3 wt.% quartz, considering a quartz content of 4 wt.% in the F4 split used and 1 wt.% in S112.

All powder specimens were prepared by a side-loading technique into a 27 mm-diameter sample holder and measured in Bragg-Brentano geometry. The three mixed layers were measured on a URD-6 (Seifert-FPM) diffractometer (CoKα radiation generated at 40 kV and 30 mA), equipped with an automatic divergence slit irradiating 15 mm sample length, diffracted-beam graphite monochromator, 0.2 mm detector slit, and a proportional counter. The measurements were performed with the following parameters: 0.02º2θ step size and 20 s counting time, total measuring time of ~1250 min, and a measured interval of 5−80º2θ.

The mixture of the I-S material with smectite was measured using a 3003TT (Seifert) diffractometer (CuKα radiation generated at 40 kV and 40 mA) equipped with an automatic divergence slit irradiating a 10 mm sample length, a diffracted-beam graphite monochromator, a 0.5 mm detector slit, and a scintillation counter. The patterns were collected from 5 to 80º2θ with a step size of 0.03º2θ and 15 s per step, which resulted in a total measuring time of 625 min.

RESULTS AND DISCUSSION

The standard deviation, σ, was declared with two significant digits in Tables 1−5, and the refined value with the same number of decimal places as σ. This high precision is justified in the case of simulated data, because the models for refinement are identical to those which were used for the simulations. The declaration of all decimal places suggests in the case of observed data an accuracy which was not obtainable for real measurements, because all crystallographic models were just an approximation of reality, but it helps to evaluate the differences between the models. σ was not declared if a refinement limit was reached. The probabilities $p60$, $p120$, $p180$, $p240$, and $p300$ are also stated in Tables 2−5, although these values were not refined directly, but derived from the refined $p0$ and $p60120$.

The R_{wp} value is declared for each refinement. The R_{wp} also depends on the measurement conditions and can only be applied directly for comparisons of refinements using the same measurement data. The comparison of results from refinements using different measurements must be seen in relation to the R_{exp} value. R_{exp} is the smallest obtainable value of R_{wp} and can be calculated from the counting statistics of the measurement (Howard and Preston, 1989).

Rietveld refinement of simulated patterns: variation of p0 from 0.333 to 1

Eight powder patterns were simulated with identical parameters (Table 2), only the proportion of 0º rotations $p0$ was varied from 0.333 to 1. $p0 = 1$ represents the ideal 1*M* polytype without non-0º rotations while the rotational disorder is maximum for $p0 = 0.333$ and all rotations occurring are equiprobable. This disorder corresponds to the $1M_d$ polytype. The other probability parameters of the simulations were chosen as $p60120 = 0$ and $pcv = 0.5$. The starting values of all refineable parameters were set to the simulation values except $p60120$ and $p0$. The starting value for $p60120$ was 0.5 and for $p0$ 0.7. The simulated pattern of the highly disordered stacking ($p0 = 0.333$) showed a broad hump in the range from 25 to 39º2θ (Figure 1a). Other peaks appear more or less symmetric. These reflections became sharper and more symmetric with increasing $p0$ value. The continuous intensity distribution between 25 and 39º2θ also evolved toward well defined peaks for $p0 = 1$ (Figure 1h). The visual inspection of the fits showed a good convergence for all refinements. Only some of the sharp-intensity maxima are not reproduced entirely correctly, especially for the simulation with $p0 = 1$. The lowest R_{wp} value of 5.88% was obtained for the refinements from $p0 = 0.333$ to 0.6. R_{wp} increased with increasing $p0$ value up to 6.29%. All refineable parameters were reproduced correctly with slight deviations, some parameters being systematically under- or overestimated. Only $p60120 = 0$ was in all cases obtained precisely, simply because this value was the lower refinement limit. The $p0$ value was always slightly overestimated; only the refinement for $p0 = 1$, which is also the upper limit, led to a smaller value.

RIETVELD REFINEMENT OF SIMULATED PATTERNS: VARIATION OF *pcv* FROM 0 TO 1

The second series of simulated powder patterns were calculated with different proportions of *cis*-vacant layers. The parameter *pcv* was varied from 0 to 1 in steps of 0.1. Again, the patterns were fitted satisfactorily (Figure 2).

https://doi.org/10.1346/CCMN.2012.0600508 Published online by Cambridge University Press

Table 1. Structural parameters for the *DIFFaX* simulations of non-basal diffraction patterns of: (a) illite, recalculated from Drits *et al.* (2006); and (b) glauconite, recalculated from Sakharov *et al.* (1990).

(a) Structural parameters of illite layers.
Lattice constants of the orthogonal unit cell

a	5.193 Å
b	8.995 Å
c	9.99 Å

Atomic positions and occupancies of the transvacant illite layer

Atom	*x*	*y*	*z*	occupancy *p*
Si	0.4863	0.1716	0.2303	0.9
^{IV}Al	0.4863	0.1716	0.2303	0.1
Fe	0.7996	0.1667	0.5000	0.1
Mg	0.7996	0.1667	0.5000	0.3
Al	0.7996	0.1667	0.5000	0.6
O1	0.4263	0.0000	0.1863	1.0
O2	0.4935	0.1910	0.3930	1.0
O3	0.7638	0.2225	0.1646	1.0
OH	0.9215	0.0000	0.3995	1.0
K	0.0000	0.0000	0.0000	0.8

(b) Structural parameters of glauconite layers
Lattice constants of the orthogonal unit cell

a	5.210 Å
b	9.024 Å
c	9.94 Å

Atomic positions and occupancies of the transvacant glauconite layer

Atom	*x*	*y*	*z*	occupancy *p*
Si	0.0080	0.3300	0.2280	0.9
^{IV}Al	0.0080	0.3300	0.2280	0.1
Fe	0.3320	0.3330	0.5000	0.1
Mg	0.3320	0.3330	0.5000	0.3
Al	0.3320	0.3330	0.5000	0.6
O1	0.4880	0.0000	0.1760	1.0
O2	0.5100	0.1810	0.3900	1.0
O3	0.7680	0.2400	0.1650	1.0
OH	0.9650	0.0000	0.3930	1.0
K	0.0000	0.0000	0.0000	0.8

All refineable parameters could once more be obtained very close to the simulation values, and also with the tendency to be either smaller or larger for all refinements (Table 3). The parameter $-t_x(cv)$ is not refineable in the case of $pcv = 0$; $-t_x(tv)$ is not refineable in the case of $pcv = 1$. $-t_x(cv)$ is slightly greater than the simulation value and $-t_x(tv)$, smaller. Both parameters showed the tendency that the difference from the simulation value became smaller if the proportion of the corresponding layer type increased. The results for R_{wp} varied in the narrow range 5.95–5.89% with the lowest values for the intermediate values of $pcv = 0.3–0.7$.

Rietveld refinement of simulated patterns: extreme starting parameters and incorrect fixations

The simulated data of the previous series using $pcv = 0.1$ was used in four refinement trials (Table 4). The first refinement was described above. The starting values were essentially similar to the simulation values except for $p60120$ and pcv. Another refinement of the same simulated data started with extreme parameters set to one limit of the refinement range. The next two refinements contained an incorrectly fixed parameter, in one case the layer shift $t_x(tv)$ and in the other, the octahedral Fe content, p(Fe).

The refinement with the standard values produced the result with the best $R_{wp} = 5.92\%$. The statistical parameters $p0$, $p60120$, and pcv were determined well. The occupancies, the lattice parameter, and $-t_x(tv)$ were also reproduced well while $-t_x(cv) = 0.3119$ was overestimated slightly. The extreme starting values of the following refinement deviated strongly from the simulation values. A comparison of the simulated pattern and the refinement pattern right before the first

https://doi.org/10.1346/CCMN.2012.0600508 Published online by Cambridge University Press

Table 2. Structural parameters for the simulation and refinement results for a series of non-basal illite patterns using $p0$ values from 0.333 to 1, declared in the corresponding column headers.

R_{exp} = 4.01%	Simul-ation	Start value	Refinement limits	R_{wp} = 5.88% $p0$ = 0.334 result	σ	R_{wp} = 5.88% $p0$ = 0.4 result	σ	R_{wp} = 5.88% $p0$ = 0.5 result	σ	R_{wp} = 5.88% $p0$ = 0.6 result	σ	R_{wp} = 5.89% $p0$ = 0.7 result	σ	R_{wp} = 5.92% $p0$ = 0.8 result	σ	R_{wp} = 5.97% $p0$ = 0.9 result	σ	R_{wp} = 6.29% $p0$ = 1 result	σ
Lattice parameter																			
a (Å)	5.193	5.193	5.1−5.2	5.193831	0.000087	5.193832	0.000087	5.193824	0.000087	5.193810	0.000087	5.193797	0.000087	5.193791	0.000087	5.193807	0.000086	5.193677	0.000085
Atomic occupancies																			
p(Fe)	0.1	0.1	0−0.7	0.0967	0.0032	0.0971	0.0032	0.0972	0.0032	0.0973	0.0031	0.0974	0.0031	0.0975	0.0031	0.0980	0.0032	0.0882	0.0033
p(K)	0.8	0.8	0.6−1	0.8018	0.0026	0.8019	0.0026	0.8021	0.0026	0.8023	0.0026	0.8023	0.0026	0.8023	0.0026	0.8022	0.0026	0.8142	0.0028
Layer shift parallel a																			
$-t_x(cv)$	0.2999	0.2999	0.26−0.32	0.3056	0.0025	0.3066	0.0022	0.3066	0.0017	0.3064	0.0014	0.3059	0.0012	0.3051	0.0011	0.30393	0.00091	0.30517	0.00077
$-t_x(tv)$	0.4008	0.4008	0.38−0.44	0.3979	0.0021	0.3985	0.0017	0.3980	0.0011	0.39759	0.00081	0.39732	0.00072	0.39736	0.00069	0.39785	0.00066	0.39580	0.00064
Probabilities																			
$p0$	varied	0.7	0.333−1	0.3392	0.0094	0.4068	0.0083	0.5045	0.0051	0.6043	0.0034	0.7051	0.0025	0.8061	0.0020	0.9077	0.0017	0.9893	0.0010
p60120	0	0.5	0−1	0		0		0		0		0		0		0		0	
p60, p180, p300				0		0		0		0		0		0		0		0	
p120, p240				0.3304		0.2966		0.2478		0.1978		0.1475		0.0969		0.0461		0.0053	
pcv	0.5	0.5	0−1	0.509	0.020	0.515	0.016	0.510	0.010	0.5064	0.0064	0.5043	0.0048	0.5032	0.0038	0.5027	0.0032	0.4948	0.0031

Table 3. Structural parameters for the simulation and refinement results for a series of non-basal illite patterns using *pcv* values from 0 to 1, declared in the corresponding column headers.

R_{exp} = 4.02%	Simul-ation	Start value	Refinement limits	R_{wp} = 5.95% *pcv* = 0 result	σ	R_{wp} = 5.92% *pcv* = 0.1 result	σ	R_{wp} = 5.91% *pcv* = 02 result	σ	R_{wp} = 5.90% *pcv* = 03 result	σ	R_{wp} = 5.89% *pcv* = 04 result	σ	R_{wp} = 5.90% *pcv* = 05 result	σ
Lattice parameter															
a (Å)	5.193	5.193	5.1–5.2	5.193919	0.000091	5.193887	0.000091	5.193851	0.000091	5.193820	0.000090	5.193802	0.000088	5.193797	0.000087
Atomic occupancies															
p(Fe)	0.1	0.1	0–0.7	0.0976	0.0031	0.0981	0.0032	0.0979	0.0032	0.0977	0.0032	0.0975	0.0032	0.0974	0.0031
p(K)	0.8	0.8	0.6–1	0.8009	0.0026	0.8012	0.0026	0.8014	0.0026	0.8018	0.0026	0.8021	0.0026	0.8023	0.0026
Layer shift parallel to *a*															
−*tx*(*cv*)	0.2999	0.2999	0.26–0.32	n.r.		0.3119	0.0060	0.3086	0.0033	0.3078	0.0023	0.307	0.0017	0.3059	0.0012
−*tx*(*tv*)	0.4008	0.4008	0.38–0.44	0.40025	0.00022	0.39959	0.00044	0.39914	0.00050	0.39854	0.00057	0.39789	0.00064	0.39732	0.00072
Probabilities															
*p*0	0.7	0.7	0.333–1	0.7086	0.0017	0.7064	0.0024	0.7060	0.0024	0.7057	0.0025	0.7054	0.0025	0.7051	0.0025
*p*60120	0	0.5	0–1	0		0		0		0		0		0	
*p*60, p180, p300				0		0		0		0		0		0	
*p*120, p240				0.1457		0.1468		0.1470		0.1472		0.1473		0.1475	
pcv	varied	0.5	0–1	0		0.1012	0.0058	0.2027	0.0055	0.3041	0.0052	0.4044	0.0050	0.5043	0.0048

R_{exp} = 4.02%	Simul-ation	Start value	Refinement limits	R_{wp} = 5.90% *pcv* = 0.6 result	σ	R_{wp} = 5.90% *pcv* = 0.7 result	σ	R_{wp} = 5.91% *pcv* = 0.8 result	σ	R_{wp} = 5.91% *pcv* = 0.9 result	σ	R_{wp} = 5.92% *pcv* = 1 result	σ
Lattice parameter													
a (Å)	5.193	5.193	5.1–5.2	5.193803	0.000085	5.193809	0.000085	5.193815	0.000084	5.193826	0.000085	5.193888	0.000084
Atomic occupancies													
p(Fe)	0.1	0.1	0–0.7	0.0973	0.0031	0.0972	0.0031	0.0973	0.0031	0.0972	0.0031	0.0977	0.0031
p(K)	0.8	0.8	0.6–1	0.8023	0.0026	0.8023	0.0026	0.8023	0.0026	0.8023	0.0026	0.8028	0.0026
Layer shift parallel to *a*													
−t_x(*cv*)	0.2999	0.2999	0.26–0.32	0.30465	0.00087	0.30358	0.00063	0.3027	0.00048	0.30205	0.00038	0.30119	0.00024
−t_x(*tv*)	0.4008	0.4008	0.38–0.44	0.39671	0.00089	0.3958	0.0013	0.3938	0.0021	0.3886	0.0047	n.r.	
Probabilities													
*p*0	0.7	0.7	0.333–1	0.7046	0.0025	0.7041	0.0025	0.7034	0.0024	0.7028	0.0023	0.7039	0.0020
*p*60120	0	0.5	0–1	0		0		0		0		0	
*p*60, *p*180, *p*300				0		0		0		0		0	
*p*120, *p*240				0.1477		0.148		0.1483		0.1486		0.14806	
pcv	varied	0.5	0–1	0.6039	0.0047	0.7035	0.0047	0.8033	0.0047	0.9033	0.0048	1	

n.r.: Not refineable, because the proportion of the corresponding component is zero.

Table 4. Structural parameters for the simulation and refinement results for a non-basal illite pattern using two different sets of starting parameters and two refinements with incorrectly fixed parameters.

R_{exp} = 4.02%			R_{wp} = 5.92% Standard start parameters			R_{wp} = 6.03% Extreme start parameters			R_{wp} = 6.37% Incorrect $-t_x(tv)$			R_{wp} = 6.60% Incorrect p(Fe)		
	Simulation	Refinement limits	start	result	σ	start	result	σ	start	result	σ	start	result	σ
Lattice parameter														
a (Å)	5.193	5.1–5.2	5.193	5.193887	0.000091	5.1	5.193899	0.000092	5.193	5.194148	0.000096	5.193	5.19438	0.00010
Atomic occupancies														
p(Fe)	0.1	0–0.7	0.1	0.0981	0.0032	0.7	0.0952	0.0033	0.1	0.1107	0.0035	**0.2**		
p(K)	0.8	0.6–1	0.8	0.8012	0.0026	0.6	0.8018	0.0027	0.8	0.8005	0.0028	0.8	0.8184	0.0030
Layer shift parallel to a														
$-t_x(cv)$	0.2999	0.26–0.32	0.2999	0.3119	0.0060	0.26	0.3009	0.0072	0.2999	0.3019	0.0034	0.2999	0.32	0.3200
$-t_x(tv)$	0.4008	0.38–0.44	0.4008	0.39959	0.00044	0.44	0.39919	0.00042	**0.41**			0.4008	0.40165	0.00047
Probabilities														
$p0$	0.7	0.333–1	0.7	0.7064	0.0024	1	0.7045	0.0024	0.7	0.7227	0.0024	0.7	0.7111	0.0028
$p60120$	0	0–1	0.5	0		1	0		0.5	0		0.5	0.0001	0.0089
$p60$, $p180$, $p300$				0			0			0			0.00001	
$p120$, $p240$				0.1468			0.1477			0.1386			0.1445	
pcv	0.1	0–1	0.5	0.1012	0.0058	1	0.0867	0.0060	0.5	0.1837	0.0044	0.5	0.1334	0.0056

Values given in bold: incorrect parameters.

Table 5. Refinement results of observed data. Results from refinements using oriented mounts from Ufer *et al.* (2012).

			Urkut, powder		oriented	ISCz-1, powder		oriented	F4, powder		oriented	67 wt.% F4 + 33 wt.% S112	
			R_{wp} = 7.31%			R_{wp} = 7.90%			R_{wp} = 5.77%			R_{wp} = 6.48%	
	Start value	Refinement limits	R_{exp} = 1.83% result	σ		R_{exp} = 2.42% result	σ		R_{exp} = 2.98% result	σ		R_{exp} = 4.62% result	σ
Global parameters													
IS (wt.%)			86.64	0.17		98.647	0.087		91.144	0.090		64.88	0.76
Quartz (wt.%)			13.36	0.17		1.353	0.087		8.856	0.090		2.015	0.088
Smectite (wt.%)												33.10	0.76
p(Fe)	0.1	0–0.7	0.429	0.012	0.4492	0.233	0.012	0.0453	0.0297	0.0061	0	0.0678	0.0091
p(K)	0.8	0.6–1	0.8349	0.0056	0.6931	0.6638	0.0051	0.6176	0.7627	0.0035	0.7017	0.7675	0.0077
Non-basal model													
a (Å)	5.193/ 5.210 (G)	5.1–5.2/5.3 (G)	5.22906	0.00029		5.19832	0.00039		5.19938	0.00070		5.20129	0.00045
$-t_x(cv)$	0.2999	0.26–0.32	0.2892	0.0032		0.26			0.2627	0.0016		0.2674	0.0027
$-t_x(tv)$	0.4008	0.38–0.44	0.38310	0.00092		0.44			0.4300	0.0017		0.4234	0.0029
*p*0	0.7	0.333–1	0.7746	0.0038		0.4962	0.0095		0.6332	0.0043		0.5926	0.0078
*p*60120	0.5	0–1	0.915	0.016		0.410	0.012		0.2342	0.0093		0.327	0.014
*p*60, *p*180, *p*300			0.0687			0.0689			0.0286			0.0444	
*p*120, *p*240			0.0096			0.1486			0.1404			0.1371	
pcv	0.5	0–1	0.2551	0.0065		0.5960	0.0072		0.5335	0.0068		0.528	0.012
Basal model													
t_s(1w) (Å)	12.5	11.65–12.85	11.65		12.85	12.688	0.038	12.85	12.285	0.022	12.85	12.156	0.059
t_s(2w) (Å)	15	14.3–15.51	14.779	0.076	14.450	15.1288	0.0091	14.9463	15.054	0.014	15.0504	14.945	0.013
p(Ca)	0.2	0.1–0.3	0.1		0.1	0.1		0.1	0.1		0.295	0.2604	0.0099
$p(H_2O)$ (1w)	0.8	0–3	3		0	0		3	1.57	0.41	2.92	3	
$p(H_2O)$ (2w)	0.6	0–3	1.71	0.76	3	2.200	0.082	2.000	1.56	0.22	2.332	2.22	0.15
$d(H_2O)$ (Å)	1.2	1.0–1.5	1.5		1.5	1.155	0.027	1.431	1.5		1.5	1.209	0.059
*w*I (R0,R1/R3)	0.5/0.875	0*–1	0.9478	0.0046	0.9616	0.6497	0.0049	0.7132	0.8745	0.0016	0.85627	0.8377	0.0033
*p*1w	0.5	0–1	0.349	0.055	0.348	0.173	0.014	0.1287	0.422	0.012	0.1283	0.184	0.020
*p*II (R1)	0	mpdo–1				0.5564	0.0053	0.5979	0.8565 (mpdo)			0.8063 (mpdo)	
*p*III (R2)		mpdo–1							0.8325 (mpdo)			0.7597 (mpdo)	
*p*IIII (R3)	0.8	mpdo–1							0.8323	0.0031	0.7890	0.7746	0.0067

* The lower refinement limit for R3 is increased due to the definition range.

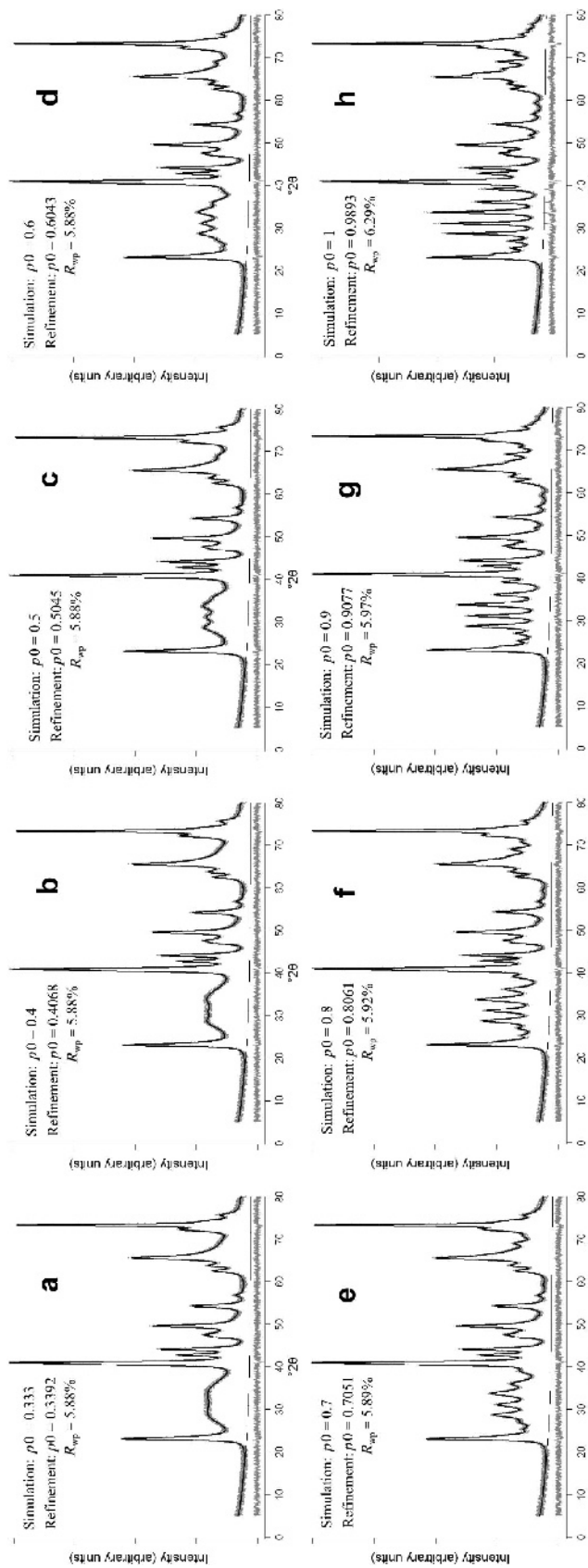

Figure 1. Simulated (gray) and refined (black) non-basal patterns of a series of illite structures varying $p0$ from 0.333 to 1. $pcv = 0.5$ and $p60120 = 0$.

https://doi.org/10.1346/CCMN.2012.0600508 Published online by Cambridge University Press

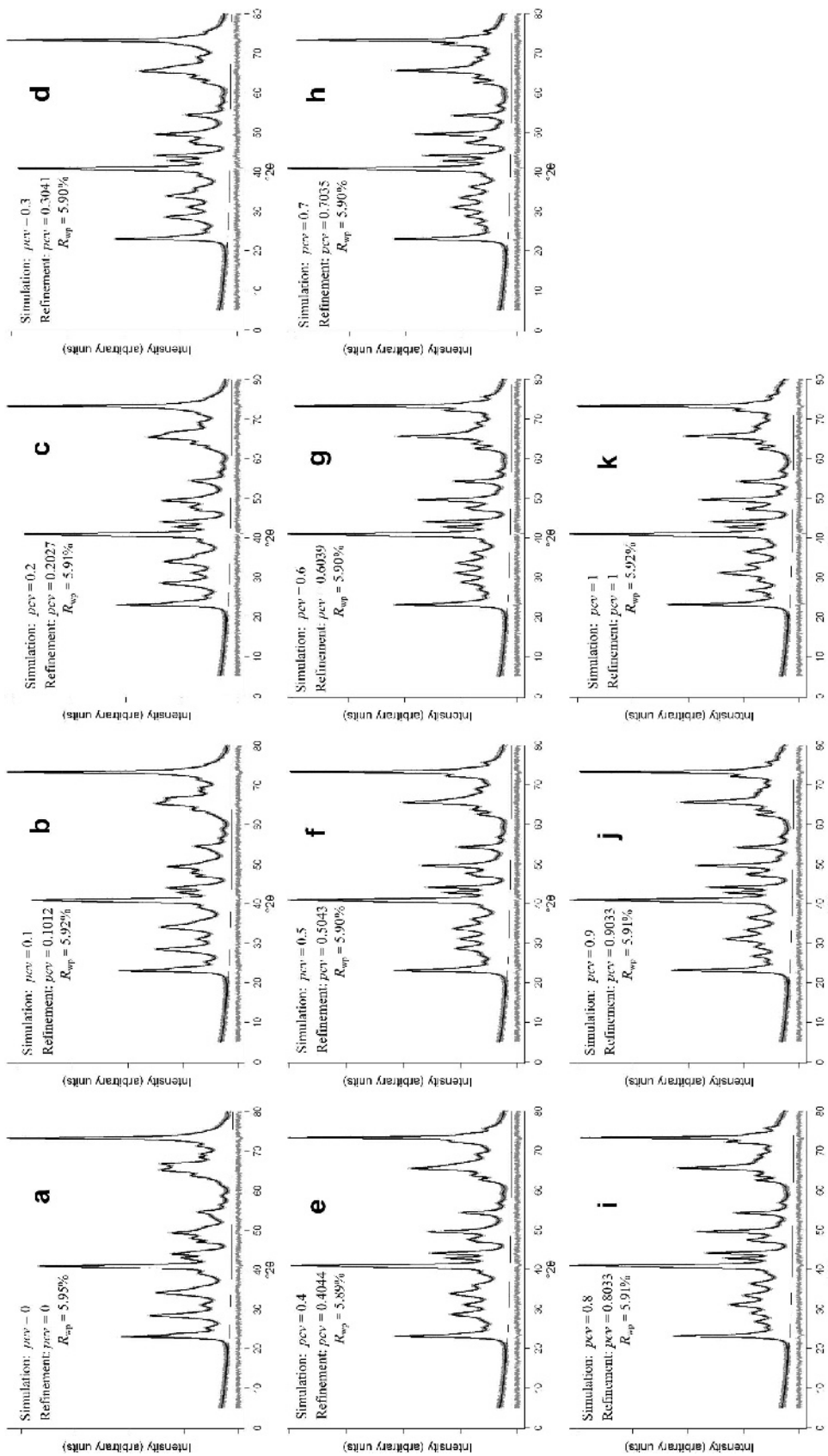

Figure 2. Simulated (gray) and refined (black) non-basal patterns of a series of illite structures varying pcv from 0 to 1. $p0 = 0.7$ and $p60120 = 0$.

https://doi.org/10.1346/CCMN.2012.0600508 Published online by Cambridge University Press

refinement cycle showed that peak positions, widths, and intensities hardly match (Figure 3, upper). Even this refinement led to a good visual agreement of the diffraction lines (Figure 3, lower) and an R_{wp} value of 6.03%, which is only 0.11% greater than the previous one. Most refined parameter values were satisfactory; only pcv = 0.0867 was slightly too small (original value 0.1). Interestingly, $-t_x(cv)$ = 0.3009 and $p0$ = 0.7045 were closer to the simulation values than in the refinement with the better R_{wp}. These two refinements showed that refinements which started with different values can result in solutions which are similar but not identical.

The use of slightly incorrectly fixed parameters led to clearly visible mismatches of the patterns and unfavorable R_{wp} values. A fixed layer shift $-t_x(tv)$ = 0.41 instead of the correct value, 0.4008, increased the R_{wp} to 6.37%. The whole pattern above 22º was affected by the incorrect parameter and showed modulated intensity differences (Figure 4, upper). The probability parameter pcv = 0.1837 was clearly larger than the simulation parameter, while the other refineable parameters are at least close to the simulation values.

The refinement using the octahedral site occupation p(Fe) = 0.2 instead of 0.1 showed a distinct intensity difference at 42.8º (Figure 4, lower). All other differences were not that pronounced. The R_{wp} was 6.60%. The occupancy of K, the other refineable parameter which influences the intensity distribution, did not really compensate the incorrect Fe content. Instead, the parameters $t_x(cv)$ and pcv disagreed. Two additional simulations were performed to evaluate the effect of

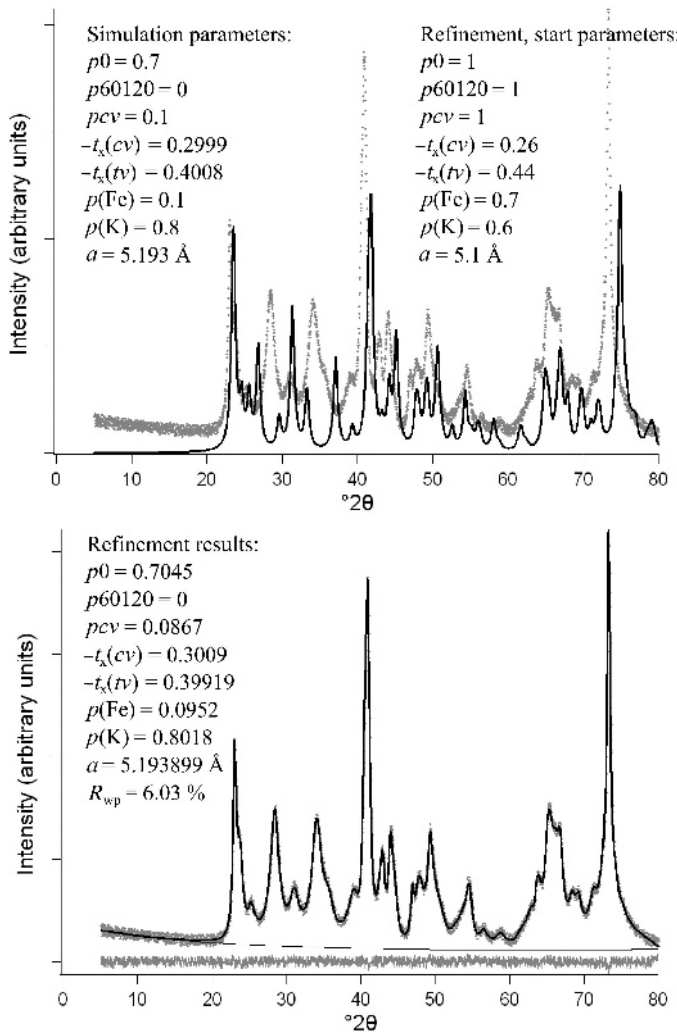

Figure 3. Simulated non-basal pattern of an illite structure with $p0 = 0.7$, $p60120 = 0$, and $pcv = 0.1$. Refinement with extreme starting values. Upper: simulated and refined pattern right before the first refinement cycle. Lower: refinement result. Gray lines – simulated patterns; black lines – refined patterns.

https://doi.org/10.1346/CCMN.2012.0600508 Published online by Cambridge University Press

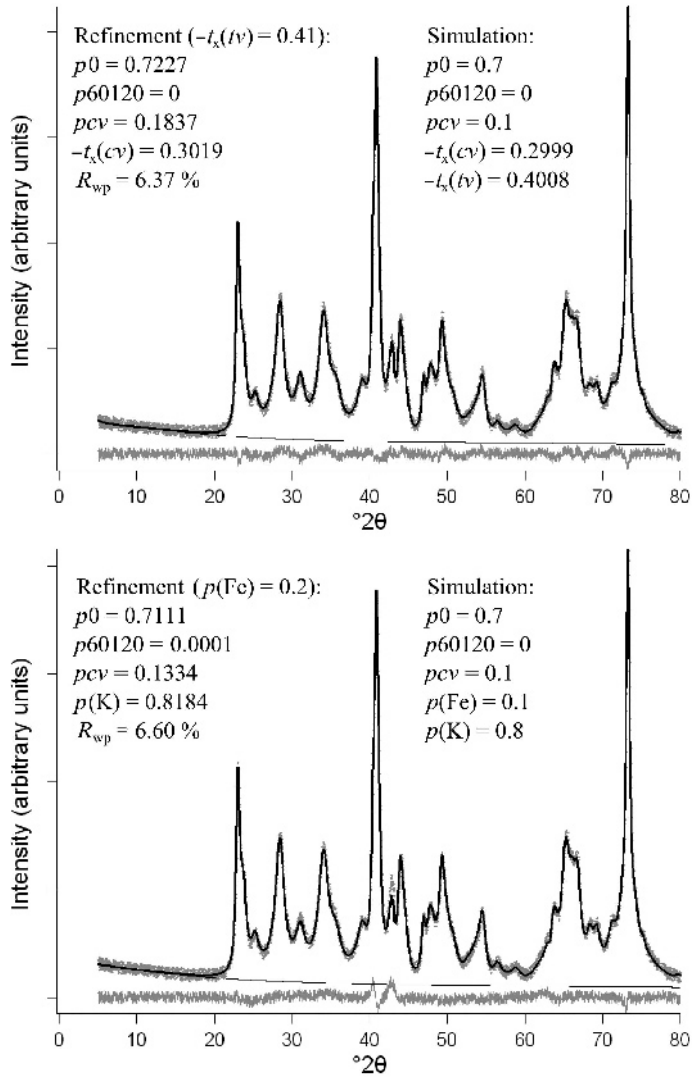

Figure 4. Simulated (gray) non-basal pattern of an illite structure with $p0 = 0.7$, $p60120 = 0$, and $pcv = 0.1$. Refinement with incorrect fixed parameters. Upper: refinement using $-t_x(tv) = 0.41$. Lower: refinement using p(Fe) = 0.2. Black lines – refined patterns.

different Fe occupancies. The two calculations were made for an illite showing $p0 = 0.5$, $p60120 = 0.5$, and $pcv = 0.5$. One of them contained 0.05 Fe atoms per position and the other, 0.25. The diffraction lines were compared directly without artificial background and instrumental noise (Figure 5). They were scaled vertically in order to minimize the difference. This comparison showed again that the main difference is the intensity mismatch at 42–43°2θ. Other differences were more broadly distributed and may be compensated by the run of the background line in case of a real measurement, *e.g.* the broad intensity hump between 22 and 40°2θ. Differences which lie in a shoulder region like that at 62°2θ can easily be compensated by a slight shift of peaks. This explains why a misfit caused by an intensity-affecting parameter also influences position-affecting parameters. In general, the effect of an incorrectly set octahedral site occupation is less obvious for the *hk* bands than is known for 00l series.

Rietveld refinement of observed data

Three different samples and one mixture were used as testing materials for the disorder model. Suitable models to describe the basal reflections were chosen according to Ufer *et al.* (2012). The choice of refineable parameters, starting values, and limits was identical to the refinements of simulated data. The results could be partially compared with the results from the refinements in Ufer *et al.* (2012) using oriented mounts (Table 5). Parameters which characterize the smectitic interlayer space are not comparable, because the samples were measured under different conditions and so the occupancies and positions of interlayer water molecules and the thickness of the smectitic layers differ.

https://doi.org/10.1346/CCMN.2012.0600508 Published online by Cambridge University Press

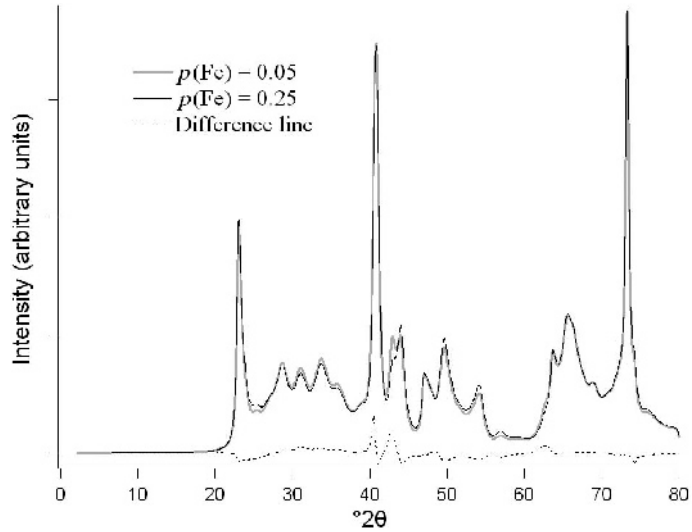

Figure 5. Comparison of two different simulated patterns of an illite structure with $p0 = 0.5$ and $p60120 = 0$ and $pcv = 0.1$. Gray line: occupancy p(Fe) = 0.05. Black line: occupancy p(Fe) = 0.25. Raw data without instrumental noise and background. Scaled vertically to minimize the difference.

The patterns of the G-S sample, Urkut, showed well resolved symmetrical peaks (Figure 6). The proportion of glauconitic layers was determined as 0.9478 while the refinement using the measurement of oriented mounts led to a slightly higher value of wI = 0.9616. The occupancy of octahedral iron p(Fe) = 0.429 came close to the expected value. Using X-ray fluorescence analysis (XRF) (Ufer *et al.* 2012) the value p(Fe) should be 0.415. This refinement result was clearly satisfactory. On the contrary, the occupancy of potassium, p(K) = 0.8349, was too large compared to 0.71, as determined by XRF. The refined values of the occupancies of the calcium and the water in the smectitic interlayer space reached the refinement limits or showed a very high standard deviation. These doubtful occupancies were almost certainly caused by the very small proportion of smectitic layers.

The result of the lattice constant a = 5.2206 Å showed an extremely small standard deviation and was in the

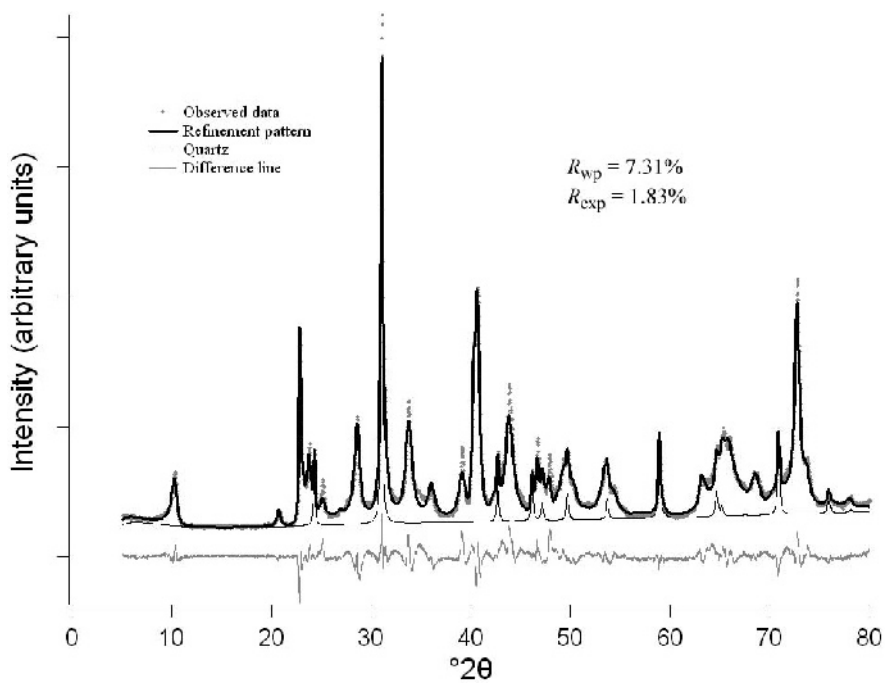

Figure 6. Refinement of Urkut sample.

https://doi.org/10.1346/CCMN.2012.0600508 Published online by Cambridge University Press

expected range for glauconites. The statistical parameters for rotational disorder showed that most layers were not rotated ($p0$ = 0.7746) and that the non-0º rotations were dominated by $n{\cdot}60º$ rotations ($p60120$ = 0.915).

The refinement of the powder pattern of sample ISCz-1 led to unsatisfactory results. The occupancy of iron p(Fe) = 0.233 was strongly overestimated in comparison to an occupancy calculated from chemical data, which is $p(Fe)_{chem}$ = 0.04. Almost this precise value was achieved in the refinement using data from oriented mounts. The previous simulations demonstrated that a discrepancy of Fe contents led to intensity misfits at 42−43º2θ. Visual inspection of the patterns indeed showed mismatches in this region, and the whole pattern also contained deviations between the refinement line and the measured line (Figure 7). Other parameters (t_x, p(Ca) and $p(H_2O)(1w)$) reached the refinement limits. The lattice constant a was again determined with a very small standard deviation. The proportion of illitic layers wI = 0.6497 was smaller than the reference value, 0.7, of the supplier. This value was better determined by the refinement using oriented mounts. Nevertheless, the inconsistent results and the significant misfit of the *hk* pattern indicate an erroneous structure model for this natural sample.

The refinement pattern of sample F4 showed a comparatively good agreement with the observed data, although minor misfits were still present at 40−50º2θ (Figure 8). Only p(Ca) and $d(H_2O)$ reached the refinement limits, but the occupations of water molecules and the thicknesses of smectitic layers had high standard deviations. The interlayer potassium p(K) (Table 5) was calculated as 0.76, significantly greater than the value obtained from the basal series only and came closer to the value of 0.79 as derived from chemical analysis (Ufer *et al.*, 2012). Octahedral iron p(Fe) was calculated as 0.03, a small value in satisfactory agreement with the chemical analysis (Ufer *et al.*, 2012). Again, the lattice parameter a showed a very small standard deviation. The stacking probabilities wI and pIIII were in good agreement with the results from the refinement using oriented mounts. Obviously, combination of the two models in a refinement on the powder pattern gave reliable values for the structural parameters for this sample.

QUANTITATIVE PHASE ANALYSIS

The results of a quantitative Rietveld phase analysis of a mixture of the illite-smectite F4 and the smectite S112 was compared with the initial composition (Table 5). Note that the automatic refinement of the mixture data included the full set of structural parameters of the I-S mineral as applied to the pure sample. Such strategy is unusual in quantitative phase analysis, as the problem of parameter correlation and convergence to wrong minimum is known to become critical in mixtures. However, the authors were interested in assessing the behavior of the full model in phase analysis. The results were in good agreement with the known contents; absolute deviations for I-S and smectite

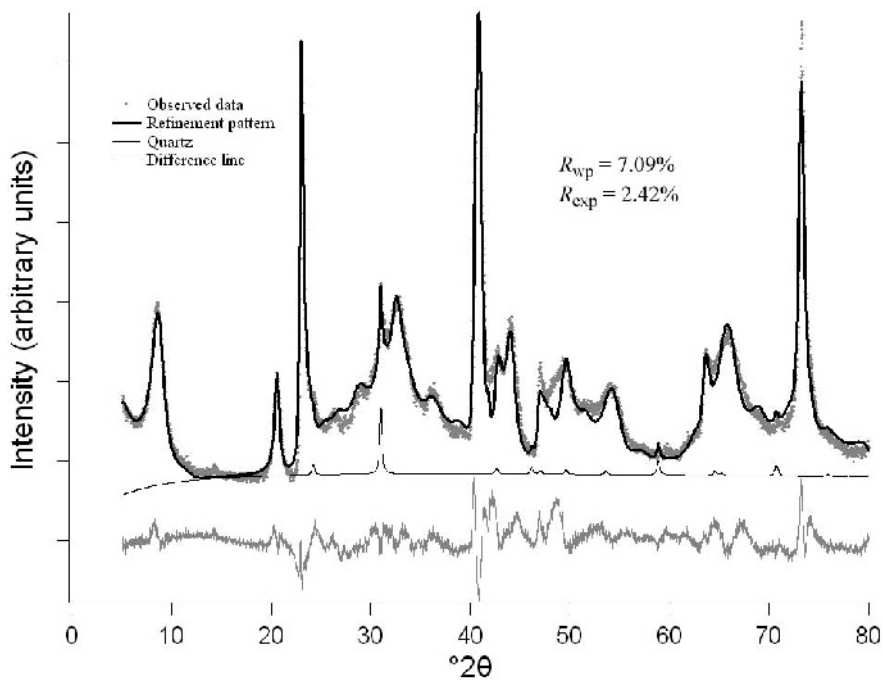

Figure 7. Refinement of sample ISCz-1.

https://doi.org/10.1346/CCMN.2012.0600508 Published online by Cambridge University Press

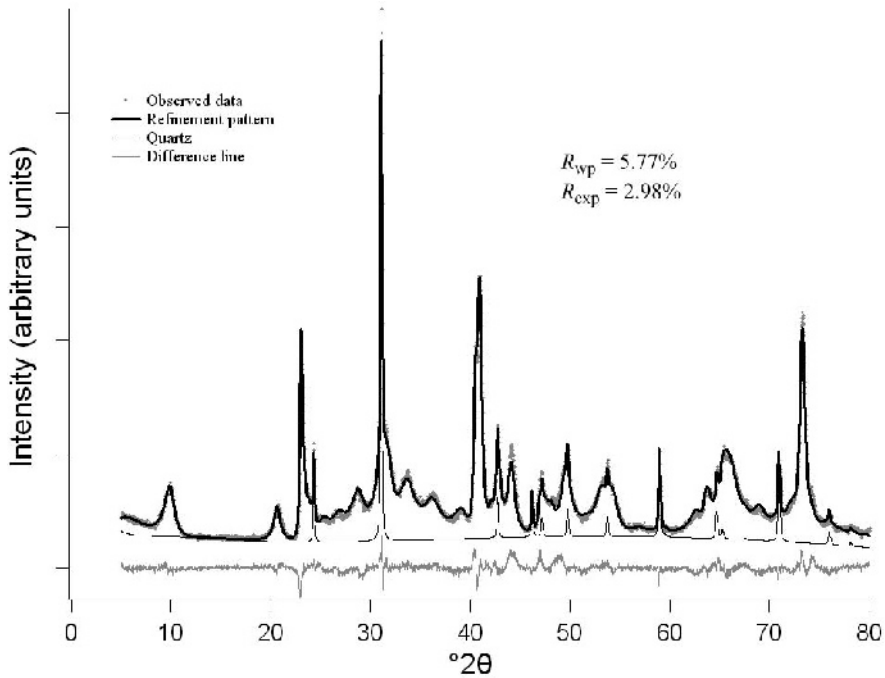

Figure 8. Refinement of sample F4.

were <1 wt.%. The I-S and smectite showed strong overlap (Figure 9) due to their structural similarity. A comparison with the refinements of the pure material showed that the statistical parameters *w*I, *p*IIII, *p*0, and *pcv* agreed or were at least in the same order of magnitude, an outcome which highlights the potential of retrieving structural information by Rietveld refinement even from powder diffraction patterns of mixtures in spite of the extreme overlap of the phase patterns of the mixed-layer mineral and the smectite.

SUMMARY AND CONCLUSIONS

The recursive treatment of diffraction from a disordered stack of layers can be combined with a Rietveld refinement and this approach can be used to obtain

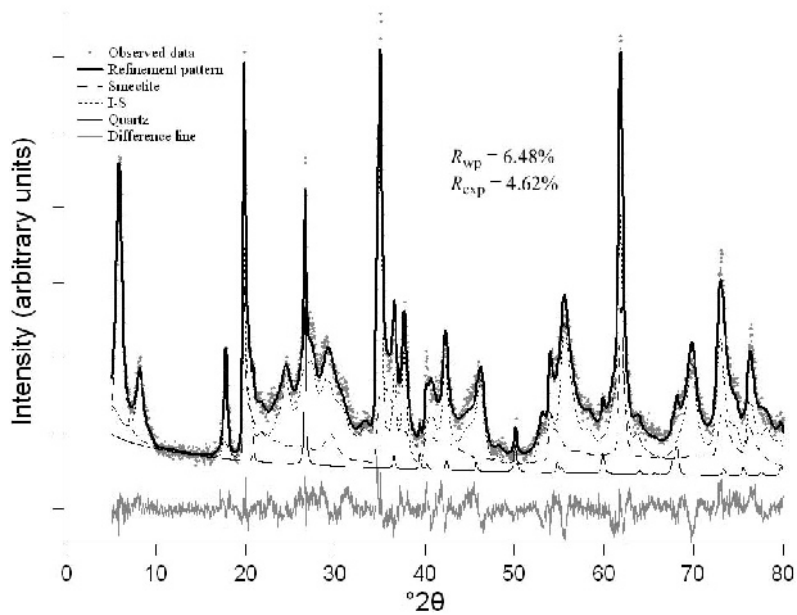

Figure 9. Refinement of a mixture of sample F4 and a smectite-rich bentonite.

https://doi.org/10.1346/CCMN.2012.0600508 Published online by Cambridge University Press

quantitative phase contents and reasonable structural parameters. Use of separate but related structural models to describe basal and non-basal reflections is necessary.

Patterns simulated with the reference software *DIFFaX* could be fitted reliably. Minor but systematic deviations of simulation parameters and refinement results were observed. Sharp peaks of slightly disordered structures showed positional misfits in some cases. The difficulties in reproducing well defined peaks arose from the use of an orthogonal supercell. This unit cell may not fit the Bragg peak positions of ordered stackings exactly. An increase in the supercell dimensions would produce more peak positions and reduce this misfit problem.

Different starting values, even extreme ones, led to similar results. This highlights the stability of the minimization algorithm. Incorrectly fixed parameters led to incorrect results for other parameters, but were not completely compensated. Misfits of the patterns and increased R_{wp} values indicate the presence of a source of errors.

Occupations of octahedral Fe and interlayer K could be reproduced reliably for simulations. In contrast, the refinement of p(Fe) failed for sample ISCz-1 and even the refinement of p(K) for the dominant illitic layers of all samples were dubious. Large standard deviations and the reaching of refinement limits of the smectitic interlayer occupancies p(Ca) and $p(H_2O)$ also demonstrated the difficulties in refining occupancies.

The Rietveld method allows the simultaneous structure-based refinement of more than one disordered phase. Quantitative phase analysis of coexisting disordered/ordered structures is possible, even though the diffraction lines of the I-S and the smectite are difficult to decompose by any user-interactive method. Separation of the intensities of all phases was possible by Rietveld refinement and information about parameters other than phase contents was also available. The refinement of structural parameters led to reasonable results by this approach. These structural results should of course be interpreted carefully.

ACKNOWLEDGMENTS

The authors are grateful to Associate Editor, Eric Ferrage, and the reviewers, Bruno Lanson and Anne-Claire Gaillot, for useful suggestions and corrections for the manuscript.

REFERENCES

Altaner, S.P. and Ylagan, R.F. (1997) Comparison of structural models of mixed-layer illite/smectite and reaction mechanisms of smectite illitization. *Clays and Clay Minerals*, **45**, 517–533.

Bergmann, J., Friedel, P., and Kleeberg, R. (1998) BGMN – a new fundamental parameter based Rietveld program for laboratory X-ray sources, its use in quantitative analysis and structure investigations. *CPD Newsletter, Commission of Powder Diffraction, International Union of Crystallography*, **20**, 5–8.

Cheary, R.W. and Coelho, A. (1992) Fundamental parameters approach to x-ray line-profile fitting. *Journal of Applied Crystallography*, **25**, 109–121.

Drits, V.A. and Sakharov, B.A. (1976) *X-ray Analysis of Mixed-layer Clay Minerals*. Nauka, Moscow (in Russian), 256 pp.

Drits, V.A. and Tchoubar, C. (1990) *X-ray Diffraction by Disordered Lamellar Structures.* Springer-Verlag, Berlin, Heidelberg.

Drits, V.A., McCarty, D.K., and Zviagina, B.B. (2006) Crystal-chemical factors responsible for the distribution of octahedral cations over *trans*- and *cis*-sites in dioctahedral 2:1 layer silicates. *Clays and Clay Minerals*, **54**, 131–152.

Howard, S.A. and Preston, K.D. (1989) Profile fitting of powder diffraction patterns. Pp. 217–275 in: *Modern Powder Diffraction* (D.L. Bish and J.E. Post, editors). Reviews in Mineralogy, **20**, Mineralogical Society of America, Washington, D.C.

MacEwan, D.M.C. (1956) Fourier transform methods for studying scattering from lamellar systems. I. A direct method for analyzing interstratified mixtures. *Kolloidzeitschrift*, **149**, 96–108.

Méring, J. (1949) L'interférence des rayons X dans les systèmes à stratification désordonnée. *Acta Crystallographica*, **2**, 371–377.

Nadeau, P.H., Wilson, M.J., McHardy, W.J., and Tait, J.M. (1984) Interstratified clays as fundamental particles. *Science*, **225**, 923–925.

Reynolds, R.C. (1992) X-ray diffraction studies of illite/smectite from rocks, <1 μm randomly oriented powders, and <1 μm oriented powder aggregates: The absence of laboratory-induced artifacts. *Clays and Clay Minerals.* **40**, 387–396.

Sakharov, B.A., Besson, G., Drits, V.A., Kameneva, M.Y., Salyn, A.L., and Smoliar, B.B. (1990) X-ray study of the nature of stacking faults in the structure of glauconites. *Clay Minerals*, **25**, 419–435.

Scarlett, N.V. and Madsen, I.C. (2006) Quantification of phases with partial or no known crystal structures. *Powder Diffraction*, **21**, 278–284.

Taylor, J.C. and Matulis C.E. (1994) A new method for Rietveld clay analysis: Part 1. Use of a universally measured standard profile for Rietveld quantification of montmorillonites. *Powder Diffraction*, **9**, 119–123.

Treacy, M.M., Newsam, J.M., and Deem, M.W. (1991) A general recursion method for calculating diffracted intensities from crystals containing planar faults. *Proceedings of the Royal Society of London*, **A433**, 499–520.

Tsipursky, S.I. and Drits, V.A. (1984) The distribution of octahedral cations in the 2:1 layers of dioctahedral smectites studied by oblique-texture electron diffraction. *Clay Minerals*, **19**, 177–193.

Ufer, K., Kleeberg, R., Bergmann, J., Curtius, H. and Dohrmann, R. (2008a) Refining real structure parameters of disordered layer structures within the Rietveld method. *Zeitschrift für Kristallographie Supplements*, **27**, 151–158.

Ufer, K., Stanjek, H., Roth, G., Dohrmann, R., and Kaufhold, S. (2008b) Quantitative phase analysis of bentonites by the Rietveld method. *Clays and Clay Minerals*, **56**, 272–282.

Ufer, K., Kleeberg, R., Bergmann, J., and Dohrmann, R. (2012) Rietveld refinement of disordered illite-smectite mixed layer structures by a recursive algorithm. I: One-dimensional patterns. *Clays and Clay Minerals*, **60**, 508–535.

Warren, B.E. (1941) X-ray diffraction in random layer lattices. *Physical Review*, **59**, 693–698.

(*Received 14 September 2011; revised 25 October 2012; Ms. 616; AE: E. Ferrage*)